07 - 10 September 2009

PROCEEDINGS

54. IWK

Internationales Wissenschaftliches Kolloquium
International Scientific Colloquium

Information Technology and Electrical Engineering - Devices and Systems, Materials and Technologies for the Future

Faculty of Electrical Engineering and Information Technology

Startseite / Index:
http://www.db-thueringen.de/servlets/DocumentServlet?id=14089

TECHNISCHE UNIVERSITÄT
ILMENAU

Impressum

Herausgeber: Der Rektor der Technischen Universität Ilmenau
Univ.-Prof. Dr. rer. nat. habil. Dr. h. c. Prof. h. c.
Peter Scharff

Redaktion: Referat Marketing
Andrea Schneider

Fakultät für Elektrotechnik und Informationstechnik
Univ.-Prof. Dr.-Ing. Frank Berger

Redaktionsschluss: 17. August 2009

Technische Realisierung (USB-Flash-Ausgabe):
Institut für Medientechnik an der TU Ilmenau
Dipl.-Ing. Christian Weigel
Dipl.-Ing. Helge Drumm

Technische Realisierung (Online-Ausgabe):
Universitätsbibliothek Ilmenau
ilmedia
Postfach 10 05 65
98684 Ilmenau

Verlag:
Verlag ISLE, Betriebsstätte des ISLE e.V.
Werner-von-Siemens-Str. 16
98693 Ilmenau

ISBN (USB-Flash-Ausgabe): 978-3-938843-45-1
ISBN (Druckausgabe der Kurzfassungen): 978-3-938843-44-4

Startseite / Index:
http://www.db-thueringen.de/servlets/DocumentServlet?id=14089

IMAGE RECONSTRUCTION WITH ITERATIVE CALBRATION ALGORITHM FOR ELECTRICAL CAPACITANCE TOMOGRAPHY

Stefan Gebhardt [1], *Gernot Scheinert* [1]

Ilmenau University of Technology (1)

ABSTRACT

The article shows an application of the OIOR algorithm for electrical capacitance tomography (ECT) with iterative calibration sequence before reconstruction [1]. The challenge is the reconstruction of several objects with unknown permittivity in a square sensing area by using always the same simulation data for calibration.

Index Terms— Capacitance measurement, Electromagnetic tomography, Image processing

1. INTRODUCTION

An Electrical Capacitance Tomography (ECT) sensor is used to calculate and image a dielectric material distribution in an observed volume with measured capacitances between sets of electrodes placed around its measuring zone. For image reconstruction, several algorithms are used [2] to image the dielectric material distribution in a definite volume being circular [3] or square [4]. They differ in speed and quality of the reconstructed image. While iterative algorithms may produce high-quality images, they are regarded as being time-consuming. We use the OIOR algorithm consisting of an iterative calibration sequence similar to Landweber algorithm [5] without concerning time consumption to the subsequent reconstruction based on Linear Back Projection (LBP). During the calibration sequence it is generated an approximated inverse sensitivity matrix **D**. The influence to the reconstruction images depending on the material distributions used to calibrate the matrix **D** is researched. With a 2D finite elements package we determine the capacitances and mathematical software is used for calculations and presentation of the results as 2D grey level images.

Typically an ECT sensor consists of a set of measuring electrodes placed outside an insulation layer with low permittivity material which surrounds the measuring area. Between each pair of the electrodes are placed guard electrodes. Enclosing the whole configuration an earthed shield reduces external electromagnetic field influences. By applying an excitation signal sequentially to one electrode and measuring to each of the remaining electrodes a set of independent capacitance data can be determined. Considering the design rules for ECT sensors, where for example the electrodes length has to be larger than the diameter of the sensor, avoids the fringe effect of the electromagnetic field in the both axial ends of the sensor. Under this consumption capacitance values computed by numerical simulation of the 2D measuring area cross-section are comparable with measurements [6], [7].

The natural relation between measured capacitances and permittivity for each pixel in the resulting image is strictly nonlinear. The coefficients describing the nonlinear system are united in a sensitivity matrix $\boldsymbol{S}$. For various image-reconstruction algorithms of ECT [4] a linear approximation (1) is used where $\boldsymbol{S}$ is the transformation matrix or linearized sensitivity matrix, $\boldsymbol{\epsilon}$ the permittivity vector and $\boldsymbol{S}$ the capacitance vector.

$$\boldsymbol{C} = \boldsymbol{S}\boldsymbol{\epsilon} \tag{1}$$

The elements $s^n_{i,j}$ of the linearized sensitivity matrix represent the sensitivity of capacitances $C_{i,j}$ between ith excitation electrode and jth measurement electrode to a small change of permittivity in the nth pixel. Capacitances are normalized by (2) where $\boldsymbol{C}_{high}$ is the set of capacitances with complete filled area by highest relative permittivity ϵ_r^{high}. $\boldsymbol{C}_{me}$ is the measured set of capacitances that needs to be normalized and the set of capacitances with the minimum permittivity distribution is expressed by $\boldsymbol{C}_{low}$.

$$\boldsymbol{\lambda} = \frac{\boldsymbol{C}_{me} - \boldsymbol{C}_{low}}{\boldsymbol{C}_{high} - \boldsymbol{C}_{low}} \tag{2}$$

$$\boldsymbol{\lambda} = \boldsymbol{S}\boldsymbol{g} \tag{3}$$

The measuring zone is virtually subdivided into a definite number of pixels m and the permittivity distribution in this zone is represented for each pixel by the image vector $\boldsymbol{g} = (g_1, g_2, ..., g_m)^T$ with minimum pixel value $g_n = 0$ (ϵ_r^{low}) and maximum pixel value $g_n = 1$ (ϵ_r^{high}). An ECT sensor with k electrodes yields in a set $\boldsymbol{\lambda}$ of $k(k-1)/2$ independent normalized capacitances $\boldsymbol{\lambda}_{i,j}$ that we can describe the system with equation (3).

Thanks to the AIF Germany for funding.

2. INVERSE PROBLEM

The goal of the reconstruction is the calculation of the image vector $\boldsymbol{g}$ from the measured set of normalized capacitances $\boldsymbol{\lambda_{me}}$ which requires the inverse of the sensitivity matrix. However the matrix S^{-1} does not exist, hence a common practice is the non-iterative Linear Back Projection (LBP) algorithm which uses the transposed matrix $\boldsymbol{S^T}$ as a rough approximation of $\boldsymbol{S^{-1}}$.

For reconstruction we use the Offline Iteration Online Reconstruction (OIOR) algorithm which produces in two stages adequate quality images in relation to the reconstruction speed by calculating in the first stage (calibration) an approximated inverse sensitivity matrix $\boldsymbol{D}$ by an iterative sequence with adaptive step-length [1]. The iterative sequence starts with the initial solution vector $\boldsymbol{g}_0$ obtained by LBP in equation (4).

$$\boldsymbol{g}_0 = \boldsymbol{D}_0 \boldsymbol{\lambda}_{in} \tag{4}$$

The matrix $\boldsymbol{D}_0$ is the transpose of the sensitivity matrix $\boldsymbol{S}$ and the vector $\boldsymbol{\lambda}$ represents the normalized capacitances of the initial permittivity distribution. To find a more adequate solution the matrix $\boldsymbol{D}$ is iteratively improved by a sequence similar to the Landweber sequence which is widely applied in optimization theory and gives (5) where $\boldsymbol{I}$ is the identity matrix and k is the number of iteration defined in the range $(0 \leq k \leq z-1)$.

$$\boldsymbol{D}_{k+1} = (\boldsymbol{I} - \alpha_k \boldsymbol{S}^T \boldsymbol{S}) \boldsymbol{D}_k \; + \; \alpha_k \boldsymbol{S}^T \tag{5}$$

$$\boldsymbol{e}_k \; = \boldsymbol{\lambda}_{in} - \boldsymbol{S} \boldsymbol{D}_k \boldsymbol{\lambda}_{in} \tag{6}$$

$$\alpha_k = \frac{\|\boldsymbol{S}^T \boldsymbol{e}_k\|}{\|\boldsymbol{S}\boldsymbol{S}^T \boldsymbol{e}_k\|_2^2} \tag{7}$$

A large number of iterations can distort the image even with decreasing error $\boldsymbol{e}_k$ [1, 5]. Hence the error vector $\boldsymbol{e}_k$ in (6) and the adaptive step-length α in (7) is calculated in each iteration step by minimizing the norm of the error vector $\boldsymbol{e}_k$ to reduce the number of iterations.

$$\hat{\boldsymbol{g}}_z = \boldsymbol{D}_z \boldsymbol{\lambda}_{me} \tag{8}$$

In the second stage (reconstruction) an image is produced by Linear Back Projection (LBP) with the capacitance vector $\boldsymbol{\lambda}_{me}$. Using the LBP with the calculated matrix $\boldsymbol{D}_z$ in (8) results the reconstruction image represented through the grey level vector $\hat{\boldsymbol{g}}$. The advantage of this algorithm is the image quality which is similar to Landweber sequence but reconstructed with the same computation time as LBP.

3. IMAGE QUALITY ESTIMATION

To estimate the reconstructed images several common criteria are possible. We use the capacitance residual (9), the image error (10) and Pearson's correlation coefficient (11) [8] between the vector $\boldsymbol{g}$ of the true permittivity distribution and the reconstructed vector $\hat{\boldsymbol{g}}$. The mean values of $\boldsymbol{g}$ and $\hat{\boldsymbol{g}}$ are given by $\bar{g}$ and $\bar{\hat{g}}$.

$$err_C = \frac{\left\| \boldsymbol{\lambda}^{ref} - \boldsymbol{D}_z \hat{\boldsymbol{g}} \right\|}{\|\boldsymbol{\lambda}\|} \tag{9}$$

$$err_I = \frac{\|\hat{\boldsymbol{g}} - \boldsymbol{g}\|}{\boldsymbol{g}} \tag{10}$$

$$\rho_{\hat{g},g} = \frac{\sum_{n=1}^{m} (\hat{g_n} - \bar{\hat{g}})(g_n - \bar{g})}{\sqrt{\sum_{n=1}^{m} (\hat{g_n} - \bar{\hat{g}})^2 \sum_{n=1}^{m} (g_n - \bar{g})^2}} \tag{11}$$

Our investigation shows that we have to use all of the three criteria to estimate the image quality because capacitance error does for instance not necessarily mean a adequate image.

4. EVALUATION BY SIMULATION

To evaluate the algorithm with accurate and almost "'noise-free"' capacitance data we use the 2-D finite elements package Ansoft Maxwell V12. Due to a needed high accuracy of capacitances, the energy error is set to 0.005% and adaptive meshing is preferred. The computation of a numerical set-up for all the sensitivity coefficients takes about 65 hours on a compute server with 2.8 GHz processor and 8GB memory.

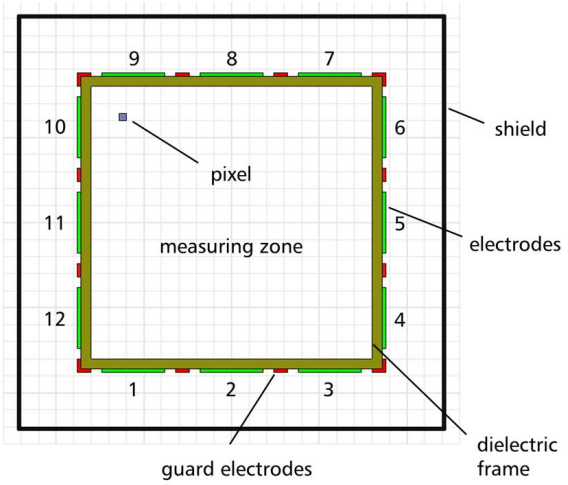

Fig. 1. Cross-section of the 12-electrode square ECT sensing area.

The square measuring zone with dimensions 80mm x 80mm is surrounded by an insulation layer with relative permittivity $\epsilon_r = 1.8$ and thickness 3mm. On the outer side of this plastic frame are located 12 electrodes where all of the electrodes are modeled with a thickness of 1mm. Between each pair of measuring electrodes is placed an earthed guard electrode. The relative permittivity of the empty space is defined to $\epsilon_r^{low} = 1$, objects and pixels are modeled completely with the maximum relative permittivity which is defined to $\epsilon_r^{high} = 2.6$. External electromagnetic field influences are reduced by an earthed shielding with dimensions 120mm x 120mm enclosing the whole setup. For each permittivity distribution results a vector $\boldsymbol{\lambda}$ with 66 normalized capacitances. Before we process the partial capacitances we have to delete selected values of the capacitance vector $\boldsymbol{\lambda}$ because directly adjacent electrodes produce some orders higher capacitance magnitudes which produce a decreasing of the image quality [9]. In our case we use 54 capacitances.

The images are calculated and presented as two-dimensional grey-scale images with Mathematica software. Subdivided into 40x40 square pixels the measuring region is defined as a uniform grid in both coordinate directions. Throughout this paper empty space of the measuring area is defined to black and the objects should be white.

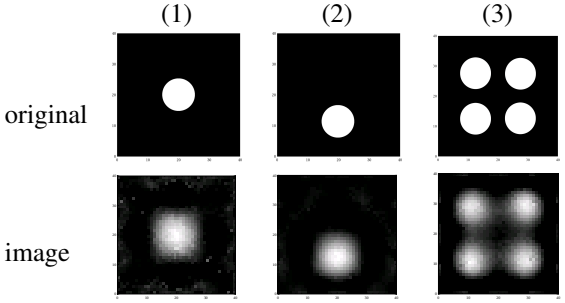

err_C	1.8233%	2.3047%	1.8497%
err_I	71.35%	55.78%	78.27%
$\rho_{\hat{g},g}$	0.7716	0.8362	0.6524

Fig. 2. Reconstruction results for different permittivity distributions in measuring area.

In Fig. 2 are shown two cases for the reconstruction of one circular rod of diameter 20mm at different positions and a third case with 4 uniformly distributed rods in the measuring area. There are the highest image errors and lowest correlation coefficients, if the objects are placed in the center area of the measuring zone. Further investigation shows the more the objects are positioned towards the edges of the zone, the more rises the image quality. The OIOR algorithm is applicated with 200 calibration steps where the initial capacitance vector $\boldsymbol{\lambda}_{in}$ is the same like the vector $\boldsymbol{\lambda}_{me}$ of the measured permittivity distribution, see original image.

In an industrial application the initial capacitance vector has to be estimated from any permittivity distribution because the observed volume is unknown. The conclusion of Liu [1] means that the algorithm is able to approach the same converged matrix $\boldsymbol{D_z}$ independent of different $\boldsymbol{C}$. So it may be interesting to compare the image results by using (7) with initial capacitance vectors $\boldsymbol{\lambda}_{in}$ of different permittivity distribution.

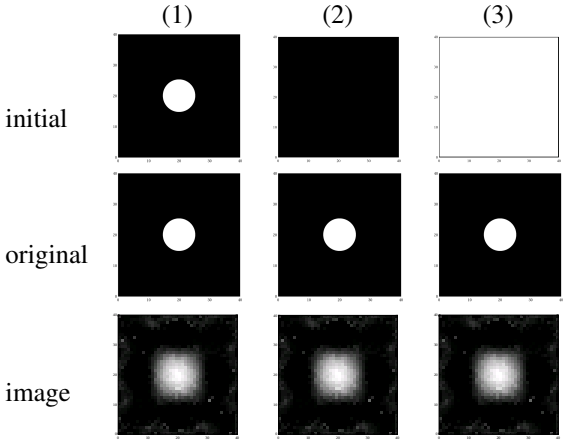

err_C	1.823%	1.745%	1.889%
err_I	71.352%	71.310%	71.383%
$\rho_{\hat{g},g}$	0.7717	0.7718	0.7716

Fig. 3. Reconstruction results for different initial permittivity distributions and same measured capacitance vector $\boldsymbol{\lambda}_{me}$ for all cases.

In our investigation different reference capacitance vectors would not create after a series of $\boldsymbol{D_k}$ a significant different converged matrix $\boldsymbol{D_z}$ so that $\boldsymbol{\lambda}_{in}$ can be different to $\boldsymbol{\lambda}_{me}$.
In Fig. 3 are shown the reconstruction results for a cylindrical object with diameter 20mm in the center of the measuring area. To calculate the improved inverse sensitivity matrix $\boldsymbol{D_z}$ in case (1) is used the same capacitance vector like $\boldsymbol{\lambda}_{me}$. In the second case the initial vector comes from the empty space and case (3) is estimated with a complete filled area of relative permittivity ϵ_r^{high}. All cases show similar images although the data of the empty area produce the lowest capacitance error. However, we have investigated the reconstruction of further distributions up to 4 objects on different positions which show the nearly same results. Thence we resume that we can applicate the image reconstruction by LBP with always the same converged matrix $\boldsymbol{D_z}$ to unknown material distributions.

For industrial applications it is interesting to estimate the positions of objects in the measuring zone. The higher the level of image reconstruction quality the

more effective are subsequent position calculations. A basic technique to improve the image quality is to use a threshold value but for different measured permittivity distributions also a different threshold value is optimal. In all cases in Fig. 4 we use a threshold value of 60% which is found empirical so the image error err_I is reduced to nearly the half and the correlation coefficients $\rho_{\hat{g},g}$ increased about 30%.

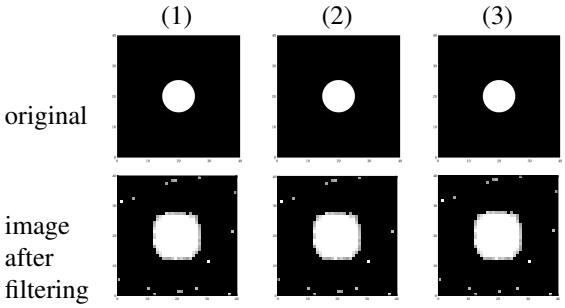

	(1)	(2)	(3)
err_C	1.823%	1.745%	1.889%
err_I	38.395%	38.396%	38.394%
$\rho_{\hat{g},g}$	0.9197	0.9197	0.9197

Fig. 4. Reconstruction results using threshold filter at 60% for different initial permittivity distributions (see Fig. 3) and same measured capacitance vector $\boldsymbol{\lambda}_{me}$ for all cases.

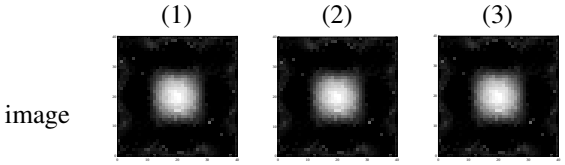

	(1)	(2)	(3)
err_C	1.744%	1.743%	1.743%
err_I	71.310%	71.318%	71.310%
$\rho_{\hat{g},g}$	0.7719	0.7718	0.7719

Fig. 5. Reconstruction results for a circular rod of diameter 20mm with different permittivity and calibration by using empty space.

Another interesting aspect is the reconstruction of objects with higher permittivity by using always the input simulation data of the empty space, because it is crucial that the method is applicable in industrial environment to objects of different dielectrical material. For the results in Fig. 5 a circular rod of diameter 20mm is defined to different relative permittivities (1) $\epsilon_r^{high} = 2.6$, (2) $\epsilon_r^{high} = 3$ and (3) $\epsilon_r^{high} = 30$. We tested the algorithm also for higher permittivities up to $\epsilon_r^{high} = 90$ with similar images for all cases.

5. CONCLUSION AND FUTURE WORK

In this work the authors show successful the application of the **O**ffline **I**teration **O**nline **R**econstruction algorithm for ECT by using different initial permittivity distributions for calibration sequence on a square measuring zone. Otherwise the algorithm enables reconstruction with always the same calibration data to unknown material distributions and objects of high permittivity.
Future research will focus on the reconstruction with primarily measured capacitances influenced on the noise due to the electromagnetic environment and the measurement electronic.

6. REFERENCES

[1] S. Liu, L. Fu, W.Q. Yang, H.G. Wang, and F. Jiang, "Prior-online iteration for image reconstruction with electrical capacitance tomography," *IEE Proc.-Sci.Meas.Technology*, vol. 151, pp. 195–200, 2004.

[2] W.Q. Yang, A.L. Stott, M.S. Beck, and C.G. Xie, "Image reconstruction algorithms for electrical capacitance tomography," *IEE Proc.-Sci.Meas. Technology*, vol. 14, pp. R1–R13, 2003.

[3] W.Q. Yang and C.G. Xie A.L. Stott, M.S. Beck, "Development of capacitance tomographic imaging systems for oil pipeline measurements," *Rev. Sci. Instrum.*, vol. 66, pp. 4326–4332, 1995.

[4] W.Q. Yang and S. Liu, "Electrical capacitance tomography with a square sensor," *Electron. Letts.*, vol. 35, pp. 295–296, 1999.

[5] L. Landweber, "An iterative formula for fredholm integral equations of the first kind," *Am. J. Math.*, vol. 73, pp. 615–624, 1951.

[6] W.Yang, "Key issues in designing capacitance tomography sensors," *IEEE sensors 2006*, pp. 497–505, October 2006.

[7] H.Yan, F.Q.Shao, H.Xu, and S.Yang, "Three-dimensional analysis of electrical capacitance tomography sensing fields," *Meas. Sci. Technol.*, vol. 10, pp. 717–725, 1999.

[8] C.G. Xie, "Experimental evaluation of capacitance tomographic flow imaging systems using physical model," *IEE Proc.*, , no. 141, pp. 357–368, 1994.

[9] S.Gebhardt and G.Scheinert, "Image reconstruction with electrical capacitance tomography and position determination of reference objects," *ITG Fachbericht 217 of XV International Symposium on Theoretical Electrical Engineering*, pp. 248–251, 2009.